Metal-based environment-sensitive MRI contrast agents

Celia Bonnet, Éva Tóth

Metal-based environment sensitive MRI contrast agents

Célia S. Bonnet and Éva Tóth

Centre de Biophysique Moléculaire, CNRS UPR 4301, rue Charles Sadron, 45071 Orléans, France

Abstract :

Interactions of paramagnetic metal complexes with their biological environment can modulate their MRI contrast enhancing properties in different ways, and this has been widely exploited to create responsive probes that can provide biochemical information. We survey progress in two rapidly growing areas: the MRI detection of biologically important metal ions, such as calcium, zinc and copper, and the use of transition metal complexes as smart MRI agents. In both fields, new imaging technologies, which take advantage of other nuclei (^{19}F) and/or paramagnetic contact shift effects, emerge beyond classical, relaxation-based applications. Most importantly, *in vivo* imaging is gaining ground and the promise of molecular MRI is becoming reality, at least for preclinical research.

Graphical abstract

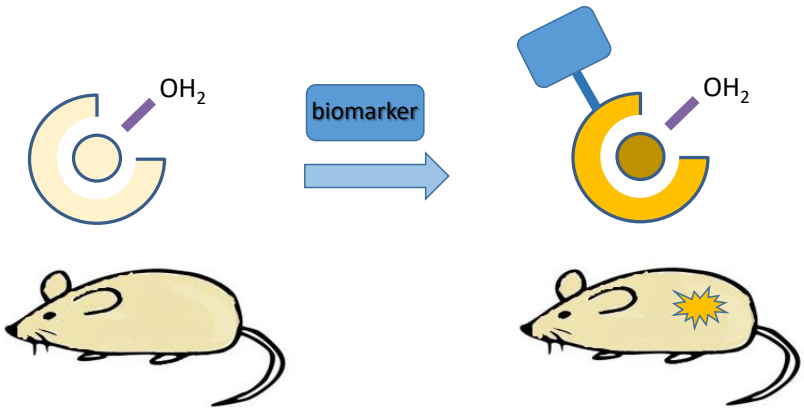

Introduction

Magnetic Resonance Imaging (MRI) has a central role in clinical radiology as well as in preclinical research, and the benefit of paramagnetic metal complexes in enhancing image contrast is well established.[1, 2] Clinical applications rely exclusively on the use of small Gd^{3+}chelates which are non-specific and reveal morphological information. Lately, there has been intensive research to derive MRI agents capable of providing biochemical information. There are two distinct approaches to achieve biochemical specificity. (i) The contrast agent can be attached to a targeting vector that recognizes a specific protein or cell type. The low sensitivity of MRI detection restricts such targeting approaches to abundant targets (μM concentrations or higher), and often requires probes with multiple Gd^{3+} centres and/or specific accumulation mechanisms at the target site. (ii) The second, "responsive" imaging approach is based on the modulation of the contrast enhancing properties of the MRI agent *via* interaction with the biological environment, thereby generating an environment-dependent signal. MRI probes are well adapted to such responsive imaging, since their contrast enhancing properties can be influenced by various biomarkers, such as tissue pH, the concentration of biologically active molecules, enzyme activities, etc. In MRI, the signal is dependent on the density and the nuclear relaxation times of tissue water protons. Through dipole-dipole interactions between the electron spin of the paramagnetic metal ion and the proton nuclear spin, the contrast agent decreases the longitudinal (T_1) and transverse (T_2) relaxation times of water protons. The efficiency of a contrast agent is given by its proton relaxivity, defined as the paramagnetic enhancement of the proton relaxation rate ($1/T_{1,2}$), induced by 1 mM concentration of the agent. Relaxivity depends on structural and dynamic parameters of the metal complex, such as the number of water molecules directly coordinated to the metal (hydration number, q), their exchange rate with bulk water (k_{ex}), and the rotational motion of the molecule (rotational correlation time, τ_R). The interaction of a responsive probe with a biomarker can affect one or more of these parameters, which will be translated into a change in relaxivity, and consequently in the MRI signal.

The last two decades have seen great chemistry efforts to conceive responsive contrast agents (also called smart or activatable),[2] although so far only few have reached *in vivo* application. Here we survey two specific areas of spectacular progress in the last years: (i) MRI detection of biologically important metal ions, where *in vivo* applications have been particularly successful, and (ii) smart agents based on transition metal complexes, which is a freshly emerging field in response to toxicity concerns associated with Gd^{3+}. In addition to relaxation agents, we will also discuss paramagnetic chemical exchange saturation (paraCEST) and shift (parashift) probes and ^{19}F MRI detection.

MRI detection of biologically important metal ions

Efforts to design cation responsive agents have focused on the detection of Ca^{2+}, Zn^{2+} and Cu^{2+}. Indeed, these three cations have important biological roles, and their misregulation has been associated to diseases such as cancer, neurodegenerative pathologies, strokes… Moreover, their *in vivo* extracellular concentrations are adapted to the low sensitivity of MRI (although Cu^{2+} is at the lower limit). For example, Ca^{2+} is present in extracellular fluids at millimolar concentrations, Zn^{2+} concentrations can reach 100 μM to mM concentrations in the pancreas and the prostate, and Cu^{2+} is at *ca.* 20 μM in blood serum. These concentrations are highly dependent of the site of interest and the physiological or pathological state.

Metal-based responsive contrast agents for cation detection are generally ditopic with distinct complexing sites for the MRI active cation (Gd^{3+}, Mn^{2+}, Ln^{3+}…) and for the cation to sense, separated

by a linker. The past years have witnessed tremendous efforts in the development of Gd^{3+}-based relaxing agents for Ca^{2+}, Zn^{2+} and, to a lesser extent, Cu^{2+}. Most of these are GdDTPA- or GdDOTA-derivatives which have shown good thermodynamic stability and kinetic inertness. Recently, with the appearance of nephrogenic systemic fibrosis,[3] macrocyclic GdDOTA derivatives displaying higher kinetic inertness have been preferred. The cation response of those agents is generally based on a switch from an *off*- to an *on*-state in terms of efficacy (relaxivity). This is generally performed by achieving: (1) *q*-change following the switch of a coordinating group from the Gd^{3+} to the cation to sense; (2) τ_R-change through self-assembly of several contrast agents around the cation to sense, or interaction with a protein, such as HSA. Evidently, the MRI active part must be thermodynamically stable and kinetically inert both in the presence and the absence of the cation to sense. This is particularly important in the case of a *q*-change as the coordination of the MRI active site varies upon interaction with the cation. Further requirements involve (i) optimized selectivity for a given cation (sometimes even a given oxidation state), (ii) affinity adapted to the local *in vivo* concentration, and (iii) reversible binding.

In the past two years, efforts to optimize and rationalize the response of relaxation agents have been pursued, but more importantly the first examples of *in vivo* applications which had emerged earlier have been really pushed forward. Several issues linked to the optimization of *in vivo* applications have been explored, such as probe quantification or the relation between cation affinity and *in vivo* response. New technologies such as fast-field-cycling MRI have been used to enhance the response at higher field. Finally, other imaging techniques relying on paraCEST, parashift agents, or ^{19}F MRI have emerged recently for cation detection.

Optimisation of Gd^{3+}-based probes for cation detection

Finding relationships between the chemical structure of contrast agents and their efficiency remains an active area of research and the ditopic character of cation responsive probes does not make the task easy. Indeed, the Gd^{3+} binding unit, the metal binding unit and the linker all play intricate roles, and predicting the coordination behavior à priori is not straightforward.[4] Towards this aim, two contrast agents for Ca^{2+} detection differing in the linker length (alkyl chain), GdL1 and GdL2 (Scheme 1), were fully characterized by NMR, luminescence measurements and DFT calculations.[5] The relaxivity changes observed upon Ca^{2+} coordination were explained by a change in the Gd^{3+}hydration state. The probe with the longer linker shows a better response to Ca^{2+} despite a smaller *q* change. NMR studies revealed different flexibility and coordination behavior upon Ca^{2+} binding, which were confirmed by DFT calculations. Dendrimeric systems of different generations (G0-G2) based on GdL3 (Scheme 1) were also studied.[6] These systems show the typical hump of slowly rotating species at medium field, and the highest relaxivity increase upon Ca^{2+} binding was obtained for the biggest dendrimers, underlying the importance of the rotational motion at medium fields.

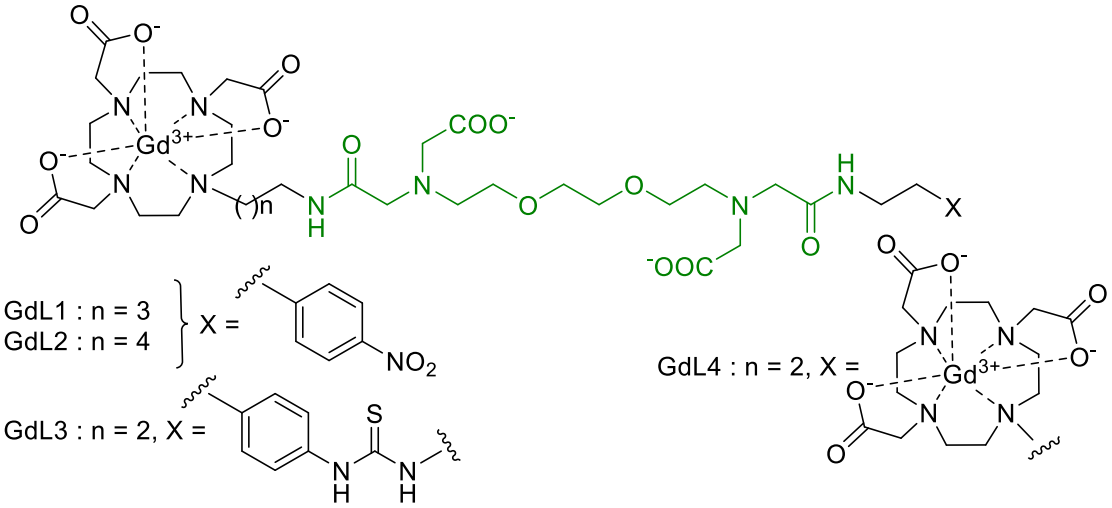

Scheme 1. Gd^{3+}-based contrast agents for Ca^{2+} detection

The role of the affinity of the metal sensing unit was investigated in Zn^{2+} detection in the case of contrast agents forming ternary complexes with HSA.[7] Inclusion of an extra methyl in the Zn^{2+} binding unit of GdL6 vs GdL5 (Scheme 2) decreased Zn^{2+} affinity by more than one order of magnitude, from 118 nM to 2350 nM, and while the *in vitro* response to Zn^{2+} in the presence of HSA at 0.5 T decreased from 200% to 100%, better *in vivo* results were observed (*vide infra*).

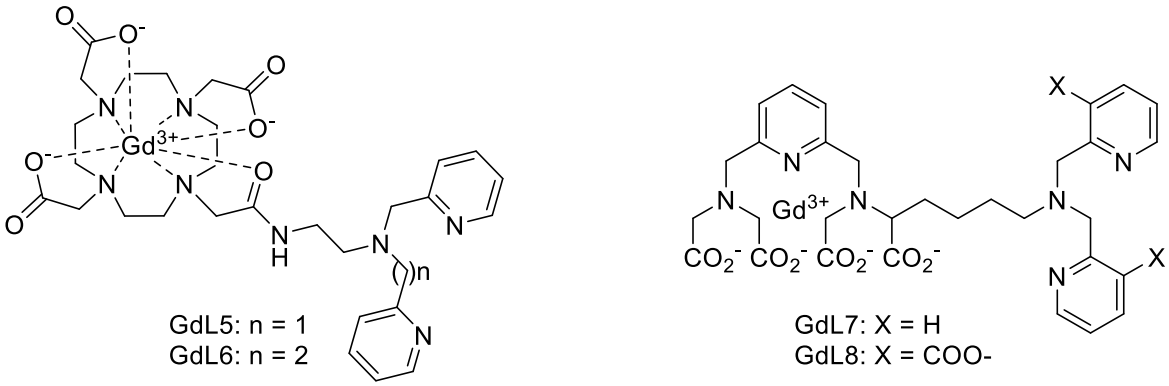

Scheme 2. Gd^{3+}-based contrast agents for Zn^{2+} detection

Bio-inspired systems represent a fundamentally different molecular design. A stable GdDOTAMA was recently attached to a zinc finger peptide (comprising 30 amino-acids) to form GdLZF (Figure 1).[8] In the absence of Zn^{2+}, zinc-finger peptides have no defined conformation. When bound to Zn^{2+}, folding occurs and the peptide adopts a compact $\beta\beta\alpha$ conformation. Zn^{2+} detection is based on this peptide conformation change: in the presence of Zn^{2+}, the originally unstructured and flexible peptide becomes compact and rigid, leading to an increased rotational correlation time, thus an increased relaxivity. The system is highly selective for Zn^{2+} vs other cations (Mg^{2+}, Cu^{2+}, Ca^{2+}, Mn^{2+} and Fe^{2+}..) with a dissociation constant in the picomolar range, and produces a relaxivity increase of 40% (37°C, 20 MHz). Moreover, the same molecule can function as a switch- *on*optical probe when Gd^{3+} is replaced by Tb^{3+}. Indeed, the tryptophan present in the peptide can sensitize Tb^{3+} luminescence through the antenna effect. In

the absence of Zn^{2+}, Trp and TbDOTAMA are too far away to observe any energy transfer, whereas upon Zn^{2+} binding, the two entities become close and energy transfer occurs, leading to a switch on luminescent signal.

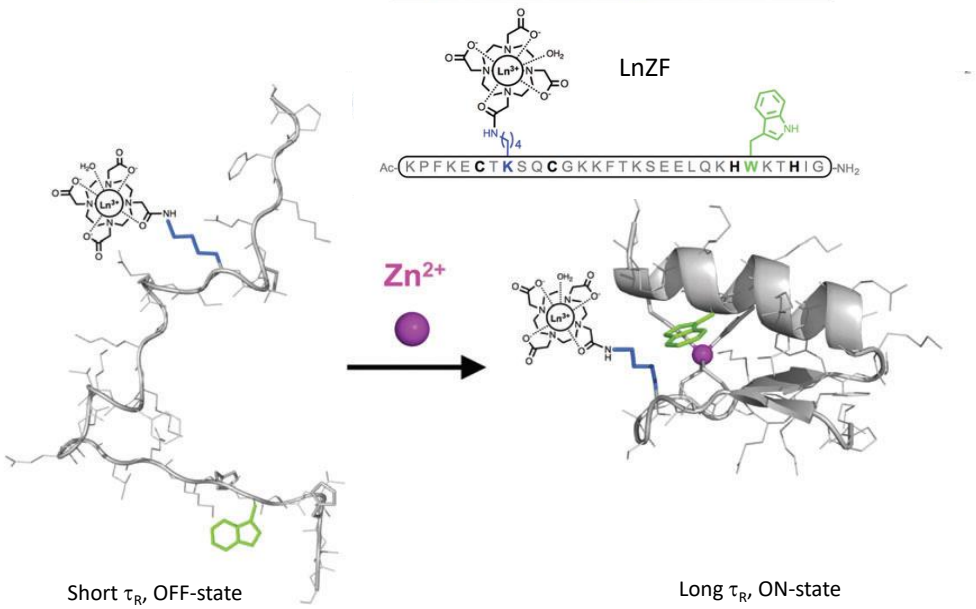

Figure 1. Bioinspired system for Zn^{2+} sensing: (top) Amino acid sequence of LnLZF; Zn^{2+}-binding cysteines and histidines are shown in black; The amino acid bearing the LnDOTAMA complex is shown in blue; The tryptophan antenna is shown in green; (Bottom) Folding of the LnZF upon Zn^{2+}-binding. Adapted with permission from Ref. [8]

FFC-MRI for cation detection

When the detection is based on *q*-change, the response is nearly similar at all frequencies. In contrast, when it relies on τ_R-changes, the relaxivity response is maximum at intermediate fields (20-80 MHz), but greatly diminishes or even vanishes at high fields. However, high-field detection is interesting due to better resolution. Fast field-cycling magnetic resonance imaging (FFC-MRI) is a novel strategy that takes specific advantage of the magnetic field dependency of relaxivity. The magnetic field is changed during the imaging sequence, while it is constant in conventional MRI. [9] Therefore the images contain information on the partial derivative of the longitudinal relaxation rate with respect to the magnetic field, $\Delta R_1/\Delta B_0$. FFC-MRI was successfully used to image probes that exhibit a strong relaxivity response upon protein binding, especially in the case of HSA.[10] We recently demonstrated its potential for Zn^{2+} detection using GdL7 (Scheme 2) which responds to Zn^{2+} in the presence of HSA. At 3T, no contrast difference is observed between phantom samples containing Zn^{2+} or not, in accordance with the similar relaxivities. In contrast, FFC MRI images show a great difference upon Zn^{2+} binding, which is consistent with the very different slopes of the NMRD curves (different $\Delta R_1/\Delta B_0$), depending on whether Zn^{2+} is present or not (Figure 2).[11] This technique is very general and applicable for the detection of any biomarker relying on a τ_R-change.

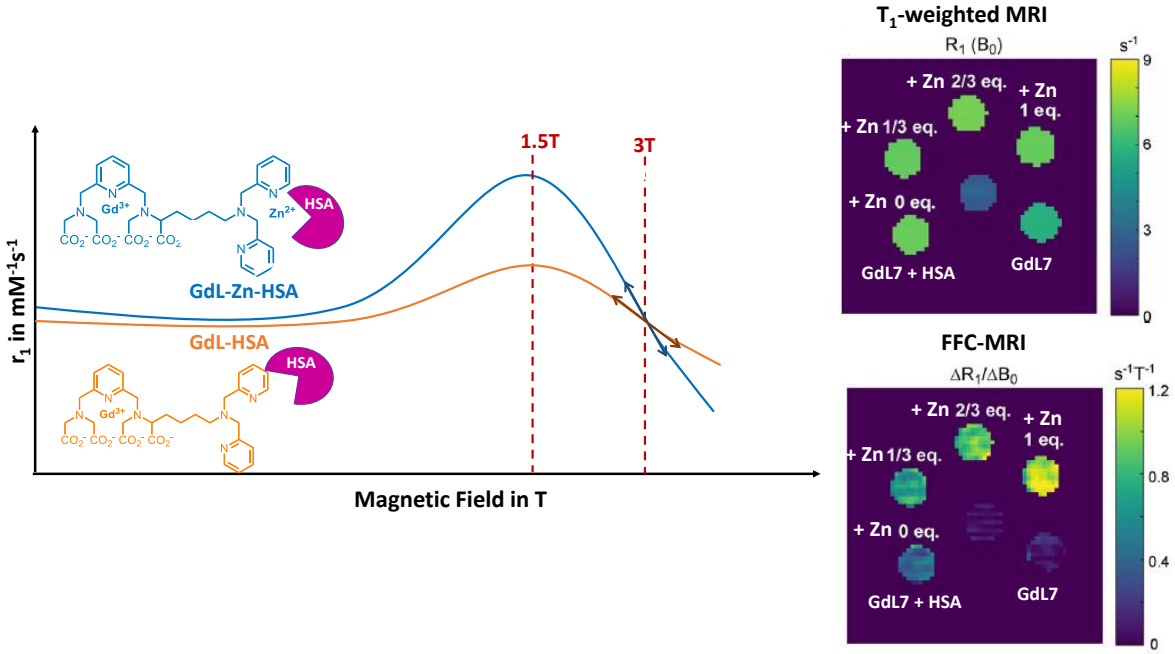

Figure 2. (Left) Schematic NMRD profiles of GdL7 with or without Zn^{2+} in the presence of HSA. (Top Right) R_1 map obtained at 2.89 T; (Bottom right) $\Delta R_1/\Delta B_0$ map obtained from substracting R_1 maps at 2.99 T and 2.79 T. Reproduced with permission from Ref [11]

In vivo applications of Ca^{2+}, Zn^{2+} and Cu^{2+} responsive probes

After the first proof of *in vivo* detection of Zn^{2+} by Sherry *et al.* in mouse pancreas following glucose stimulation ,[12] *in vivo* applications of metal-responsive contrast agents have flourished. A dinuclear Gd^{3+} complex bearing a central Ca^{2+} detection unit (GdL4, Scheme 1) has been proposed for early diagnosis and monitoring of cerebral ischemia.[13] Extracellular Ca^{2+} concentration decreases dramatically upon ischemia, but returns to its initial state if reperfusion is quickly established. By using the reversible Ca^{2+}-binding probe in a cerebral artery occlusion experimental protocol, the authors demonstrated clear signal decrease with submillimeter spatial and second-scale temporal resolution on the functional MRI images of mice.

In vivo Zn^{2+} detection is another active area of MRI research, and due to their high Zn^{2+} content, pancreas and prostate imaging attract most attention. In both organs, the important intracellular Zn^{2+} concentrations can be released into the extracellular media upon glucose stimulation. It has been evidenced by MRI that the Zn^{2+} levels released are different in healthy *vs.* malignant mouse prostate,[14] or in the pancreas of healthy mice *vs*. those with type I diabetes or with a high-fat diet.[12] The *in vivo* response in the pancreas of GdL5 and GdL6 (Scheme 2) with different Zn^{2+} affinities (see above) was studied. It is clear from Figure 3 that glucose stimulation gives a better contrast in line with the Zn^{2+} release. Following glucose stimulation, the low-affinity agent (GdL6) produced better image contrast, which could be explained by a lower background produced by endogenous Zn^{2+} prior to glucose stimulation and a better response to further Zn^{2+} increase.[7] Gd^{3+} from GdL6 and Zn^{2+} release were also quantified by synchrotron radiation X-ray fluorescence measurements in a mouse model of prostate cancer development.[15] Zn^{2+} loss was observed in the lateral lobe of the mouse prostate, the area where Zn^{2+} accumulates the most. The concomitant measurement of Gd^{3+} concentrations confirmed that glucose initiates Zn^{2+} secretion from intracellular compartments of the prostate to the extracellular media where it binds to the responsive contrast agent. Interestingly, Gd^{3+}

content in the prostate was different whether the mouse was healthy or not/ has been injected with glucose or not, pointing to the importance of quantification of such smart probes (*vide infra*).

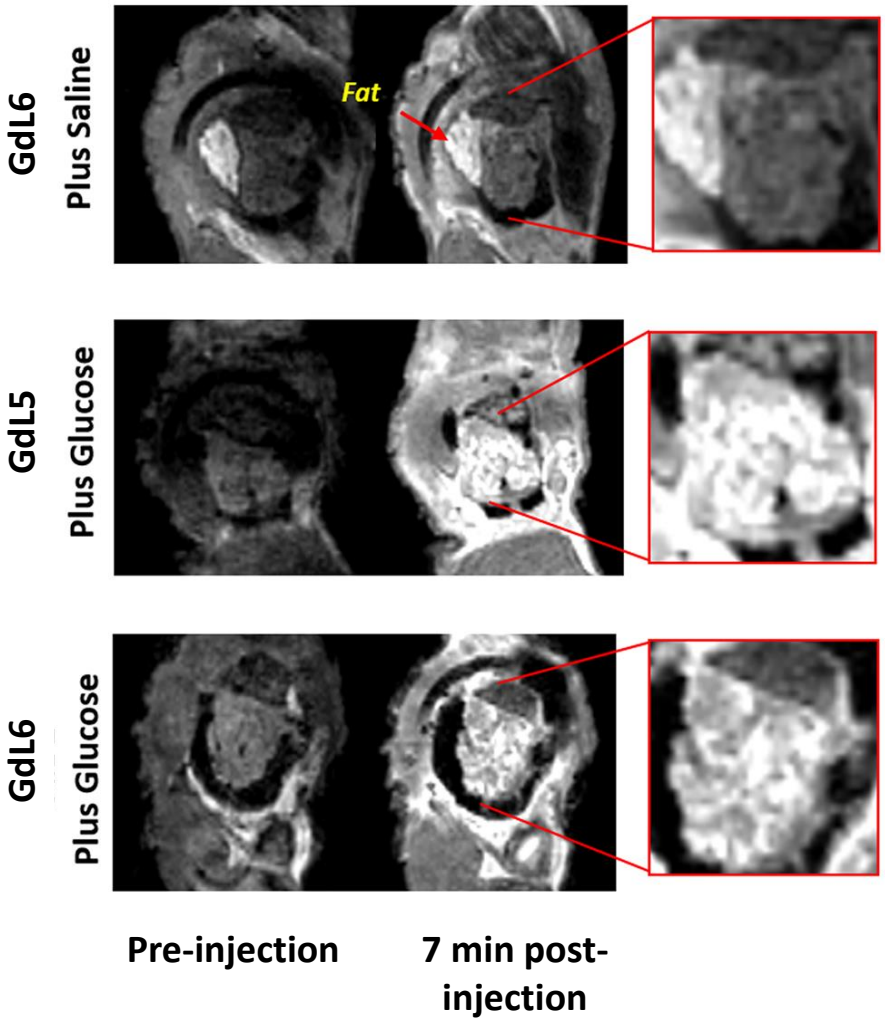

Figure 3. T_1-weighted MR images of mouse pancreas pre or post-injection of GdL5 or GdL6 plus saline or glucose (for Zn^{2+} release). Reproduced with permission from Ref [7]

Due to its lower *in vivo* concentration, Cu^{2+} detection is more challenging. One *in vivo* example of detecting Cu^{2+} excess in the mouse liver was recently reported using GdL9 (Scheme 3). Upon Cu^{2+} binding and in the presence of HSA, the contrast agent shows 270% relaxivity increase at 20 MHz .[16] EPR and XANES results show limited differences between the Cu-HSA and GdL9-Cu-HSA complexes pointing to weak interactions between the GdL9 and the Cu-HSA complex, which is consistent with the much higher Cu^{2+} affinity of HSA (K_d ≈ 0.1 pM *vs.* K_d = 84 µM for GdL9-Cu). At 4.7 T, contrast enhancement was 25% in the mice liver upon contrast agent injection, whereas it was lower when mice were treated with a Cu^{2+} chelator. This correlates well with ICP results showing similar Gd^{3+} quantities in both types of mice, while the Cu^{2+} content is half in mice treated with the Cu^{2+} chelator. An interesting addition to this study would be to ascertain that Zn^{2+} content is not altered, as the same contrast agent also responds, to a lesser extent, to Zn^{2+}, and Zn^{2+} generally has higher concentration than Cu^{2+}.

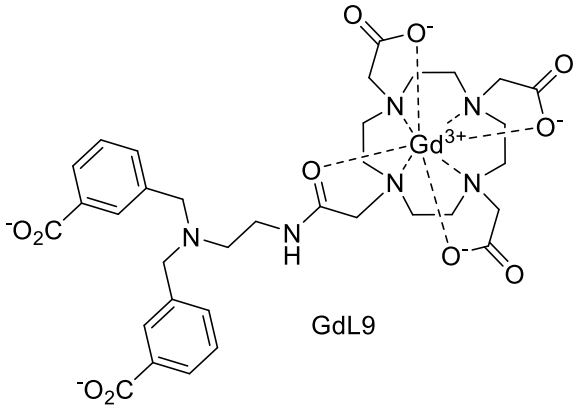

Scheme 3. Gd^{3+}-based contrast agent for Cu^{2+} detection

Quantification of the contrast agent

MRI signal intensity depends on both the local concentration of the agent (which is not known *in vivo*), and its relaxivity response to the cation. Most *in vivo* imaging studies (except for those which monitor temporal changes) typically compare signal intensities measured in healthy and sick animals/tissues; however, the biodistribution of the agent might be different in physiological *vs* pathological tissues. In order to disentangle the observed signal changes from potential variation in the local concentration of the agent, it is compulsory to develop quantitative methods for MRI detection. In the case of relaxation agents, a complementary quantitative method needs to be implemented.

We recently provided the first proof-of-concept of *in vitro* zinc quantification, by combining MRI with Single Photon Emission Computed Tomography, a quantitative nuclear imaging technique. A Gd^{3+} contrast agent sensitive to Zn^{2+} in the presence of HSA was developed (GdL8, Scheme 2).[17] Using the chemical similarity of Ln^{3+} ions, we looked for a Ln^{3+} isotope that can be visualized by nuclear techniques. ^{165}Er has an ideal half-life of 10.36 h and is readily obtained from a cyclotron. Indispensable for reliable quantification, it can be purified from the parent nucleus ^{165}Ho. We used a cocktail of the Gd^{3+} and the $^{165}Er^{3+}$ complex (of known $^{165}Er/Gd$ ratio and respecting the sensitivity of each technique) in the presence of HSA, to which unknown Zn^{2+} concentrations were added. The activity of each sample was measured using γ-spectrometry and the samples were imaged with a γ-camera. This allows for the determination of $^{165}Er^{3+}$ and consequently, Gd^{3+} concentration. In MRI, the samples were then imaged at 3 T which allowed determining accurately the Zn^{2+} content using a calibration curve. Zn2+ concentrations were then checked by independent ICP measurements. These encouraging results have now to be proven *in vivo*.

This approach was supported recently by another Ln surrogate; the positron emitter ^{86}Y was used to quantify the whole-body distribution of a Gd^{3+} contrast agent.[18]

^{19}F NMR was also used to quantify Ca^{2+}-responsive Gd^{3+} complexes. In a micelle composed of a surfactant and an amphiphilic Gd^{3+} complex responsive to Ca^{2+}, perfluoro-15-crown-5-ether was incorporated and its ^{19}F signal used as a reporter of Gd^{3+} concentration.[19] First, it was checked that Ca^{2+} binding does not affect ^{19}F MR images, while it leads to a significant increase in ^{1}H r_1 and r_2 (30 and 343 %, respectively at 7 T and 25 °C). *In vivo* MRI studies were performed after intracranial injection of the paramagnetic micelle in the somatosensory cortex of rats, using a vial of TFA for external ^{19}F calibration. The good ^{19}F signal enabled the calculation of local Gd^{3+} concentrations. An interesting addition to this work would have been to use the fluorinated micelle itself for the external calibration

(instead of TFA), as the presence of the paramagnetic ion might affect the calibration. Last but not least, once injected, the integrity of the micelle is not entirely known.

Other Ln^{3+}-based contrast agents: paraCEST, parashift and ^{19}F contrast agents

Paramagnetic hyperfine shifts induced by Ln^{3+} ions other than Gd^{3+} have been also exploited. Only few paraCEST agents have been reported for cation detection, probably due to the difficulty to predict and rationalize CEST effects. Their design relies on the modulation of the concentration or the exchange of labile protons (amine, alcohol, amide, hydration water). When these protons are selectively saturated, their chemical exchange with bulk water leads to an intensity decrease of the water peak, which can be translated to a CEST image.

Two Tm^{3+} complexes (TmL10 and TmL11, Scheme 4) were proposed as ON/OFF responsive paraCEST MRI probes for Zn^{2+} and Cu^{2+} detection.[20] The paraCEST effect originates from the amide protons which disappears upon the formation of $(TmL)_2Zn^{2+}$, $(TmL)_2Cu^{2+}$ or $(TmL)Cu^{+}$ complexes. Obviously, the system is poorly selective and the switch off CEST signal remains a difficulty for practical application.

Parashift MRI probes and their *in vivo* use is an emerging field.[21] A proof of concept of Zn^{2+} detection was achieved by chemical shift modification upon Zn^{2+} binding to LnL12 (Scheme 4).[22] A *tert*-butyl group comprising 9 protons on the ligand serves as parashift reporter in the Tb, Dy and Tm complexes with chemical shifts of -30.2 ppm, -36.5 ppm, and +17 ppm, respectively. After Zn^{2+} addition, new *tert*-butyl peaks appear with greatly decreased relaxation rates, probably resulting from the longer distance between *tert*-butyl protons and the paramagnetic centre. Zn^{2+} concentration changes could also be followed by luminescence titration of the Eu^{3+} analogue, showing important modification in the Eu^{3+} coordination sphere: Eu^{3+} is non-hydrated in the absence, and becomes monohydrated in the presence of Zn^{2+}.

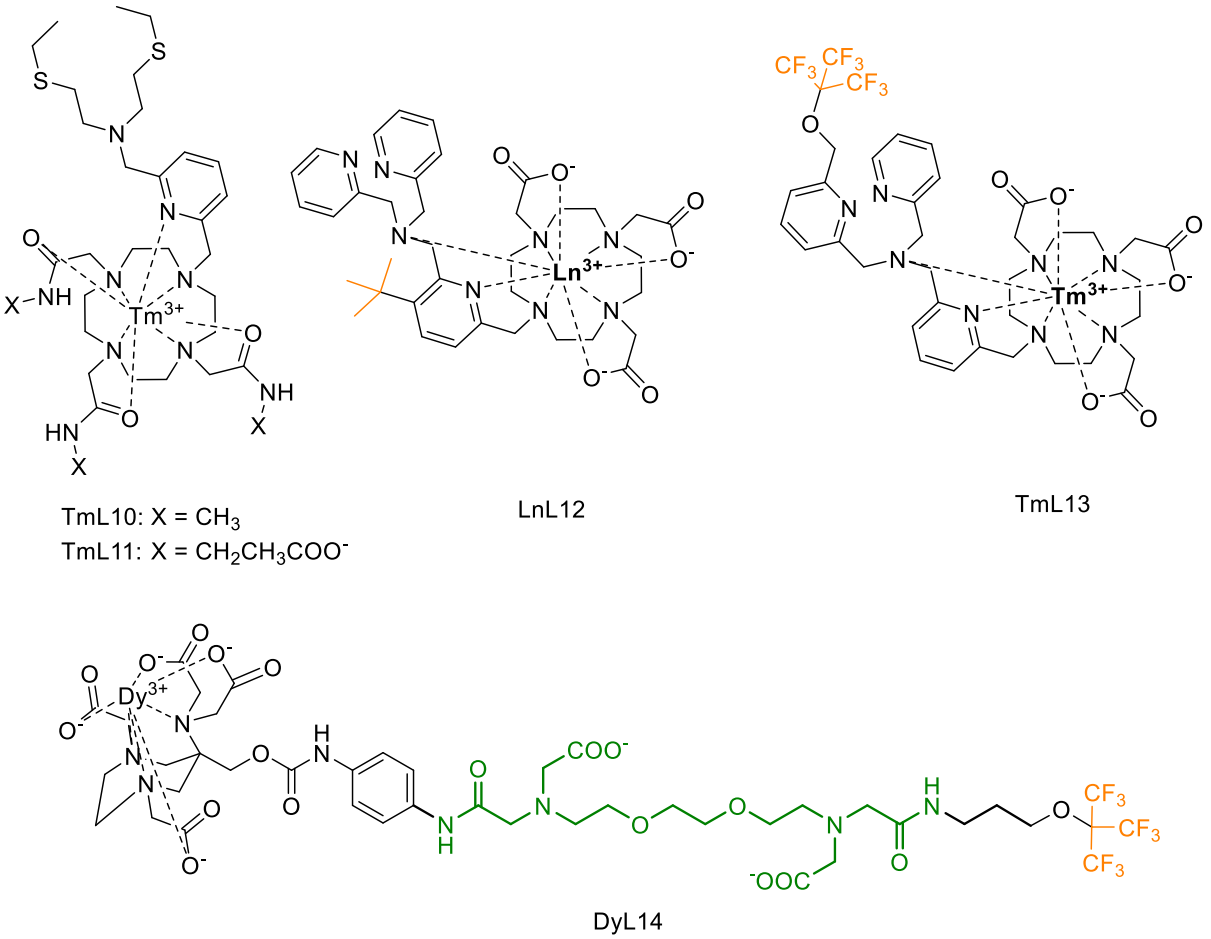

Scheme 4. ParaCEST, parashift and ^{19}F contrast agents for cation detection

^{19}F MRI has been exploited with fluorinated paramagnetic Ln^{3+} complexes. TmL13 (Scheme 4) functions as an *off/on* probe for Zn^{2+} detection.[23] In the absence of Zn^{2+}, the system is highly flexible and no ^{19}F signal is observed. Upon Zn^{2+} coordination, one major and three minor signals appear corresponding to different diastereoisomers of the probe. Zn^{2+} could be detected with ^{19}F MRI, with a detection limit of 180 µM *in vitro*.

"Frequency-encoding" of these techniques makes quantification easier, as shown for the Ca^{2+} responsive ^{19}F probe. A DyAAZTA complex, labelled with 9 fluorine atoms (DyL14, Scheme 4), was chosen because it shows a single ^{19}F signal due to the absence of isomers.[24] Upon Ca^{2+} coordination, the ^{19}F atoms come closer to the paramagnetic centre resulting in a shift of their resonance and a shortened T_1. The use of an Y^{3+} analog, insensitive to Ca^{2+}, enabled probe quantification.

Responsive agents based on transition metal complexes

Gd^{3+}-based agents were considered as safe drugs until the identification of the Gd-related disease, nephrogenic systemic fibrosis,[3] and the discovery of Gd^{3+} retention in the brain and bones.[25] All this raised health concerns about Gd^{3+} agents and promoted research towards safer and more biocompatible alternatives. Based on their capacity to enhance nuclear relaxation, high spin transition metal ions like Mn^{2+} ($S = 5/2$), Mn^{3+} ($S = 2$), Fe^{3+} ($S = 5/2$) or Fe^{2+} ($S = 3$) are the best adapted,[26] though Fe^{2+} is often ruled out due to its fast, less favorable electron spin relaxation. Manganese and iron are essential elements, but would be toxic at the quantities required for MRI examinations. Therefore,

only their stable and inert complexes can be considered for *in vivo* use. High thermodynamic stability and kinetic inertness is particularly challenging to achieve for Mn^{2+}, although recent results on rigidified ligands based on cyclohexyl diamine,[27] pyclen[28, 29] or bispidine[30] scaffolds are encouraging and these Mn^{2+} complexes likely fulfil the criteria for safe *in vivo* use. Typically, Fe^{3+} complexes are thermodynamically more stable, however, less is known about their kinetic inertness. Concerning responsive probes, in addition to the usual mechanisms to modulate relaxivity (via changes in the hydration state, water exchange or rotational dynamics), redox activity and potential spin transitions of transition metals offer additional opportunities, a versatility which makes this emerging field particularly exciting.

Relaxation agents

Mn^{2+} chelates

In the past, several responsive Mn^{2+} systems were reported to release free Mn^{2+} upon interaction with a biomarker, thus produce a relaxometric response to pH,[31] enzymes,[32] Ca^{2+},[33] or Zn^{2+}.[34] Partial decoordination of the ligand occurs also in the Mn^{2+}(qtp2) complex formed with a redox-active ligand containing quinol subunits, reported as an H_2O_2 responsive agent (Scheme 5).[35] H_2O_2 oxidizes quinols to *para*-quinones leading to their decoordination from Mn^{2+}. Thus the hydration number of Mn^{2+} changes from 0.9 to 2.8, with a concomitant relaxivity increase from 5.46 to 7.17 $mM^{-1}s^{-1}$ (3 T). EPR data evidenced that the redox process involves only the ligand and Mn retains its 2+ oxidation state.

Tircso *et al.* reported the first highly stable and inert Mn^{2+} complex which can be activated by pH change, in the biologically significant pH range.[28] The kinetic inertness of Mn(PC2A-EA) (Scheme 5) is among the highest reported for a monohydrated Mn^{2+} chelate (dissociation half-life of $t_{1/2}$=8×10^3 h; pH=7.4). As long as the ethyleneamine function is protonated in Mn(PC2A-EA) (logK_H = 6.88), it is not coordinated to Mn^{2+} and the relaxivity is high (3.54 $mM^{-1}s^{-1}$) in this monohydrated state. Following deprotonation, the coordinating amine replaces the hydration water (q = 0), and the relaxivity drops (2.04 $mM^{-1}s^{-1}$, 0.49 T, 25 °C).

A nanogel matrix containing pyridine functions served as polydentate chelator for Mn^{2+} in a polymeric pH sensor.[36] At acidic pH (≈4), the polymer swells and water molecules enter the nanogel, resulting in a significant decrease of T_1 and T_2 relaxation times. The system produces rapid pH response, observable on MRI phantoms at low (μM) Mn^{2+} concentrations; however, the swelling process still needs to be tuned to occur around physiological pH.

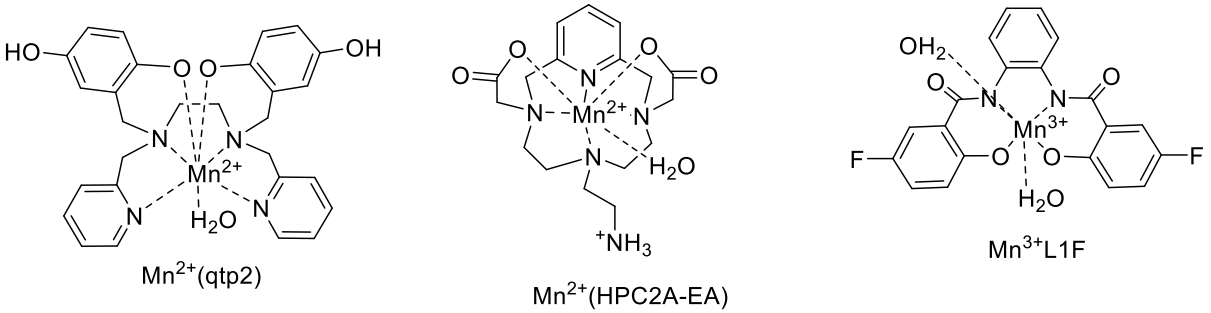

Scheme 5. Mn^{2+}- and Mn^{3+}-based responsive probes

Mn^{3+} chelates

After porphyrins which were most investigated for Mn^{3+} complexation in the context of MRI, Jasanoff *et al.* developed another promising ligand family using the 1,2-phenyldiamine bis(amidate) (PDA) skeleton. Advantages of Mn^{3+}-PDA chelates involve good relaxation efficacy, comparable to that of Gd^{3+} agents, spontaneous cell internalization and cytosolic localization.[37] Cell accumulation can be further promoted by attaching ester groups to the ligand which are cleavable by intracellular enzymes, giving rise to cellular entrapment of the complex and robust MRI signal enhancement.

To develop an intracellular Ca^{2+} sensor, the specific Ca^{2+} chelator BAPTA (BAPTA = 1,2-bis(2-aminophenoxy)ethane-N,N,N'N'-tetraacetate) was linked to the PDA backbone.[38] The acid functions of BAPTA were converted to acetomethoxyl-esters in order to maintain high cell permeability and create a probe which will respond to Ca^{2+} exclusively after cell internalization and ester cleavage by intracellular esterases. In a cell study, this ManICS1-AM probe produced MRI signal variation as a response to Ca^{2+} concentration changes which were provoked by pharmacological or optogenetic tools. These changes were confirmed by readouts from optical calcium indicators. When directly infused into the rat brain, ManICS1-AM allowed successful MRI monitoring of neural activation in deep tissues which are not accessible to optical detection (Figure 4). Although further refinement of the calcium affinity as well as the application of brain delivery strategies might be necessary, this probe already enables MRI detection of neural responses to multiple biologically relevant stimuli, at the molecular level and without depth limitation.

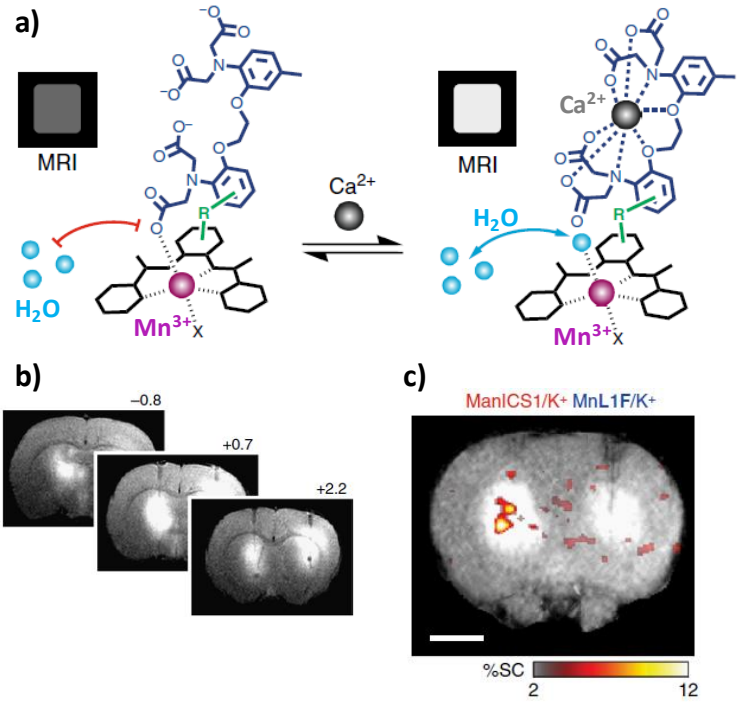

Figure 4. Calcium responsive Mn^{3+} probe ManICS1-AM: (**a**) Ca^{2+} binding to the BAPTA unit leads to increased hydration number, thus increased T_1-weighted MRI signal (7T). (**b**) *in vivo* T_1-weighted MRI (7T) showing contrast enhancement after infusion of ManICS-1 (left) or calcium-insensitive control agent (MnL1F, right) into rat striatum; (**c**) T_1-weighted MRI signal increase upon K^+ infusion in the presence of preinjected ManICS1-AM (left) but not of MnL1F (right). Adapted with permission from ref.[38]

The same group reported a fluorinated PDA derivative, MnL1F (Scheme 5) for NO detection.[39] Nitric oxide is an important signalling molecule and neurotransmitter. *In vivo* detection of this gaseous molecule is difficult due to its short lifetime and tissue diffusion. In MnL1F, NO is expected to axially coordinate to Mn^{3+}, reducing water accessibility. This was supported by the decrease of ^{17}O linewidths measured in a MnL1F solution in the presence of NO. Upon NO binding, the relaxivity decrease amounts to 22 % in water, but becomes more important in the presence of cytosolic macromolecules due to protein binding of the probe. In the future, protein binding could be further improved by attaching specific groups to the ligand to increase probe sensitivity. MnL1F was successfully used to detect NO production *in vitro* in cells expressing NO synthase and in antigen-stimulated macrophages, as well as *in vivo* in the brain using a rat neuroinflammation model. By assuming stoichiometric and irreversible binding of NO to the probe, the authors could even estimate NO production rates.

$Mn^{2+}/^{3+}$ redox switches

Both 2+ and 3+ Mn oxidation states are accessible under biological conditions. Mn^{3+} is usually a less efficient relaxation agent given its faster longitudinal electronic relaxation, but the relaxivity ratio between the two oxidation states is strongly field-dependent.[40] At higher magnetic fields, the difference can be magnified by slowing down the rotation of the system, which has a more important effect on the relaxivity for Mn^{2+} than for Mn^{3+} chelates. This was exploited to create the very first redox-active, potential MRI agent twenty years ago. The Mn^{2+}TPPS (Scheme 6) interacts with poly-β-cyclodextrin and this slowly rotating adduct shows a relaxivity decrease from 40.8 to 15.2 $mM^{-1}s^{-1}$ (20 MHz, 25°C) when the partial oxygen pressure, pO_2 increases from 0 to 40 torr and the complex is oxidized.[41] Other porphyrin- and phthalocyanine-complexes[42] have been later explored. For instance, in aqueous solution the fluorinated and PEGylated Mn-porphyrin Mn-TPFPP (Scheme 6) can reversibly switch between Mn^{3+}/Mn^{2+} oxidation states under the effect of oxygen/ascorbic acid, leading to a 2.4-fold relaxivity increase upon reduction at clinically relevant magnetic fields.[43] Interestingly, glutathione or cysteine do not reduce Mn^{3+} which makes this probe specific for ascorbic acid. It has fast reduction and slow re-oxidation kinetics and low toxicity at concentrations relevant for MRI.

Caravan *et al.* reported open-chain ligands capable of chelating Mn in both oxidation states. The hexadentate HBET and CyHBET ligands form monohydrated complexes with Mn^{2+}, while Mn^{3+} analogues are non-hydrated due to the smaller size of the oxidized form of the metal ion. Thanks to this *q*-change, up to 8-fold relaxivity increase was achievable upon Mn^{3+}/Mn^{2+} transformation (1.4 T, 37°C). The same group designed the Janus chelator JED (Scheme 6) which can adapt its coordination mode to the redox state of manganese by switching between the coordination of pyridine or phenolate groups for Mn^{2+} and Mn^{3+}, respectively.[44] Consequently, JED is able to support stable complexes of both Mn^{3+} and Mn^{2+} in biological milieu. Rapid redox interconversion is triggered by H_2O_2/peroxidase (oxidation) and *L*-cysteine (reduction), with a concomitant 5-6-fold relaxivity increase (depending on the magnetic field) from the non-hydrated Mn^{3+} to the monohydrated Mn^{2+} form. Due to protein binding of the complexes, the relaxivity response increases to 9-fold in blood plasma.

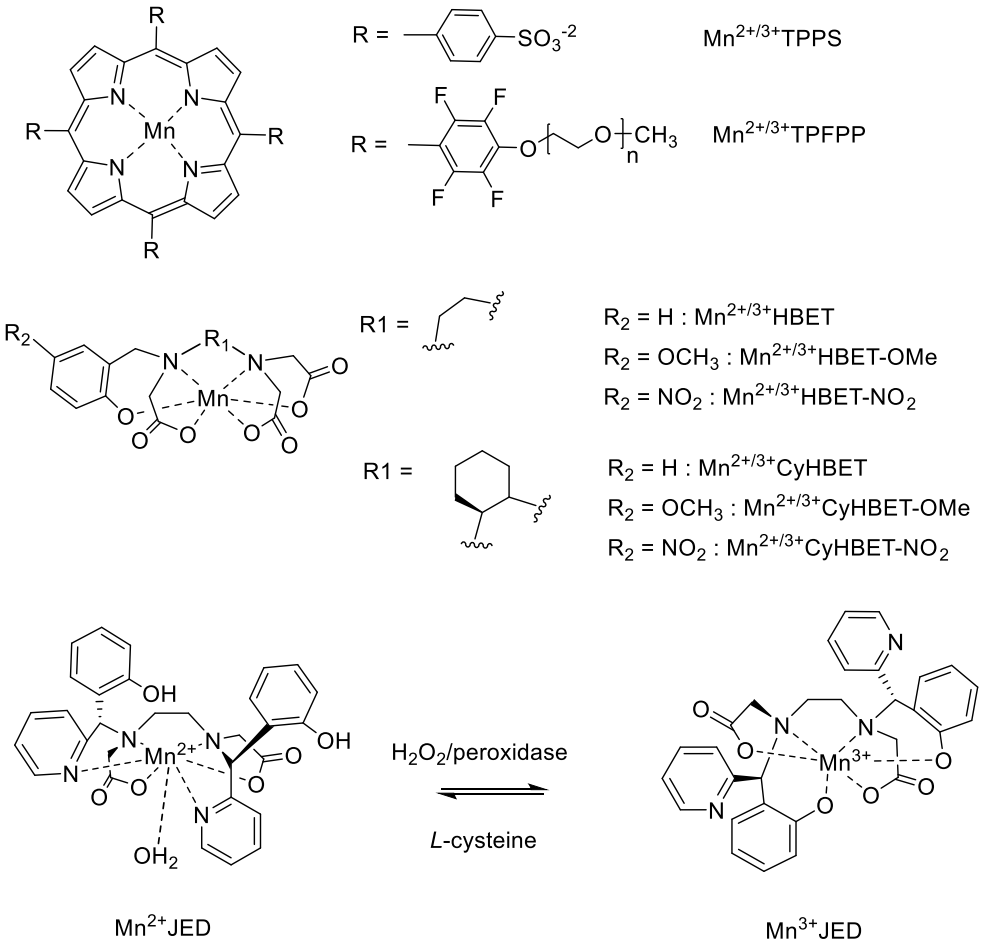

Scheme 6. Redox switches based on manganese

Iron complexes

Analogously to Mn^{2+} complexes which release the free metal ion when they interact with a biomarker, the pH-sensitive Fe^{3+}ZDS chelate (Scheme 7) partially dissociates under weakly acidic conditions, hence generating an increased MRI signal intensity.[45] ZDS is a zwitterionic dopamine sulfonate ligand with a catechol donor group that forms FeL_x complexes, where x=1-3 depending on pH. Between pH 7.4 and 5.0, the relaxivity of this complex increases from 1.6 to 3.2 $mM^{-1}s^{-1}$, resulting from ZDS decomplexation, thus increasing hydration number. This probe was used to highlight the more acidic pH of solid tumors *in vivo* in mice.

Gale *et al.* exploited the redox properties of iron to visualize elevated levels of reactive oxygen species in inflamed pancreatic tissue of a mouse model.[46] Upon oxidation of Fe^{2+}PyC3A to Fe^{3+}PyC3A (Scheme 7) with H_2O_2, the relaxivity increase is between 10- and 15-fold (at 1.4 and 11.7T, respectively). After injection of Fe^{2+}PyC3A into mice, no MRI signal enhancement is observable in normal pancreatic tissue. In diseased tissue, the hyperintense signal indicates inflammation, in good correlation with the presence of the pro-inflammatory biomarker myeloperoxidase, quantified *ex vivo*.

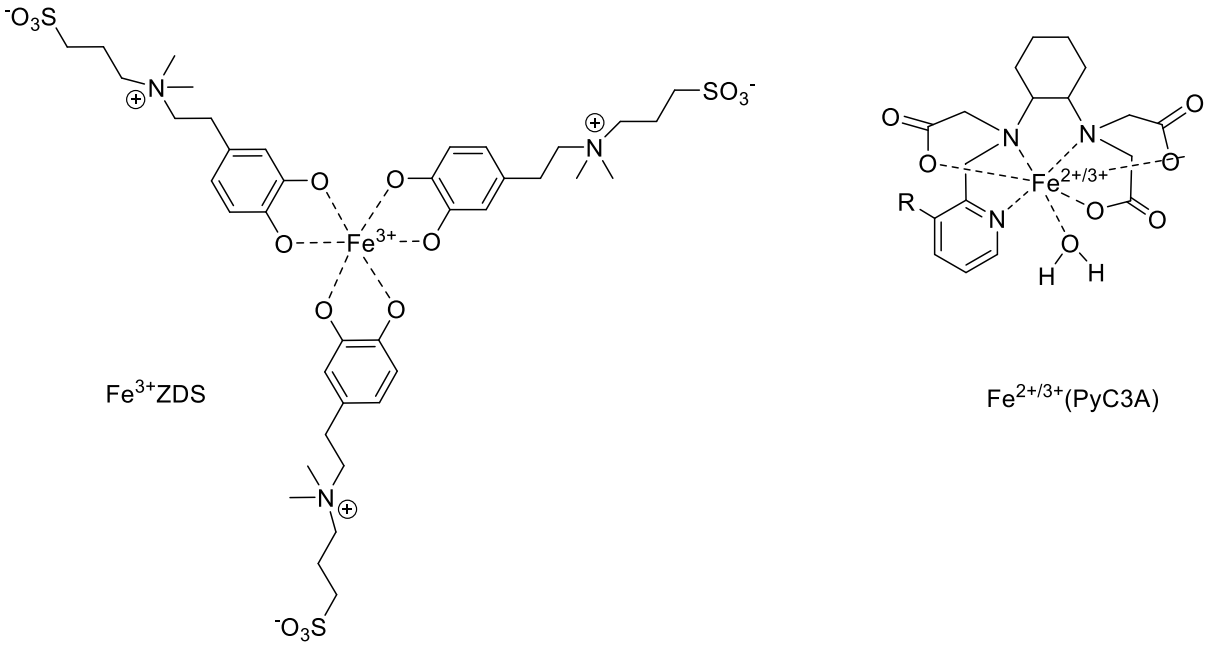

Scheme 7. Responsive iron-based probes

ParaCEST agents

High spin Fe^{2+}, Co^{2+}, or Ni^{2+} generate important paramagnetic shifts with limited relaxation effect, which makes their complexes adapted for paraCEST detection, and they are increasingly explored as responsive agents. CEST relies on proton exchange which is intrinsically dependent on pH. Although CEST suffers from low detection sensitivity, it offers the advantage of ratiometric approaches and easier quantification. The amide protons of the Co^{2+}CCRM complex (Scheme 8) generate strong, pH dependent CEST effects allowing for ratiometric pH readout, and importantly, the kinetic inertness of this *trans* isomer is very good for a Co^{2+} chelate.[47] In a different approach, the ^{19}F MRI signal of a Fe^{2+}DOTAM chelate decorated with 4 CF_3 units was used for probe quantification and ratiometric pH determination.[48] To improve pH sensitivity, Harris *et al.* incorporated two distinct ligand scaffolds in a single, dinuclear Co^{2+}L15-editronate complex (Scheme 8).[49] Proton exchange on the two ligands, a tetra(carboxamide)-derivative and a bisphosphonate, is respectively base- and proton-catalyzed. This leads to two CEST effects with opposing pH dependences, thus an amplified change of their ratio with pH. This complex is stable in physiological environments. The pH obtained from phantom images was in excellent agreement with electrode pH measurements. The same two ligands were used to form redox-responsive dinuclear Fe complexes.[50] The $(Fe^{2+})_2$ and $Fe^{2+}Fe^{3+}$ complexes are stable, inert. They provide strongly shifted, multiple, non-overlapping CEST effects adapted to ratiometric quantification of the redox potential defined by thiol-based reductants and reactive oxygen species-based oxidants.

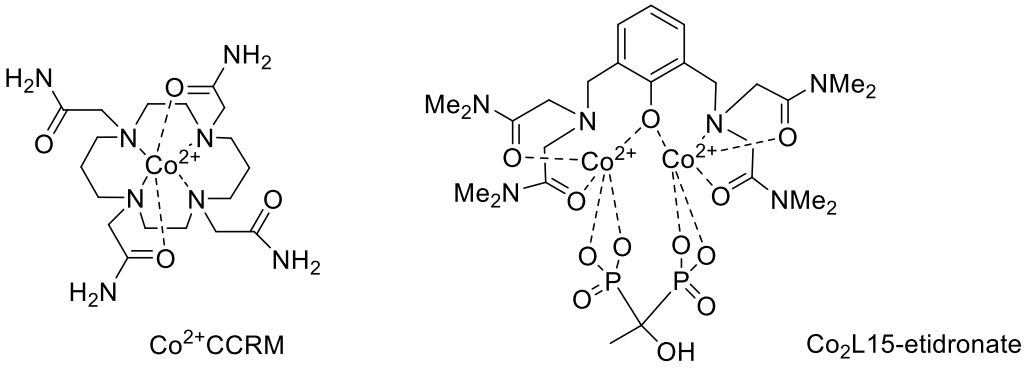

Scheme 8. Responsive paraCEST probes based on cobalt

^{19}F NMR probes

Variation in the spin state of 3d transition metals and the subsequent change in paramagnetic relaxation enhancement or pseudocontact shifts are exploited by the group of Que to derive responsive ^{19}F MRI agents.[51] Most early work focused on redox sensing. Biochemical reduction of fluorinated versions of Cu^{2+}ATSM results in a turn-*on* ^{19}F signal (Scheme 9).[52, 53] In the presence of the strong relaxation agent Cu^{2+}, the ^{19}F signal is not detectable, but it becomes visible once Cu^{2+} is reduced in hypoxic cells and the Cu^{+} complex dissociates. Cyclam-derivative Cu complexes have been also studied.[54] Fluorinated TACN complexes of the Co^{2+}/Co^{3+} couple (Scheme 9) allowed ROS detection.[55, 56] The oxidation of the highly paramagnetic, high-spin Co^{2+} to low-spin, diamagnetic Co^{3+} is translated by longer ^{19}F relaxation times, sharper ^{19}F signals and smaller chemical shifts.

The same group reported recently a new platform of spin state switching Ni^{2+} complexes for biosensing in ^{19}F MRI, with a proof of concept cell imaging study.[57] The Ni^{2+} complexes formed with side-bridged cyclam ligands (Figure 5) can be activated by light or enzymatic cleavage. The switch from the diamagnetic $S = 0$ to the paramagnetic $S = 1$ configuration of Ni^{2+} is induced by the transformation of the ligand from a 4-dentate to a 5-dentate coordination mode and results in large changes in the ^{19}F chemical shifts.

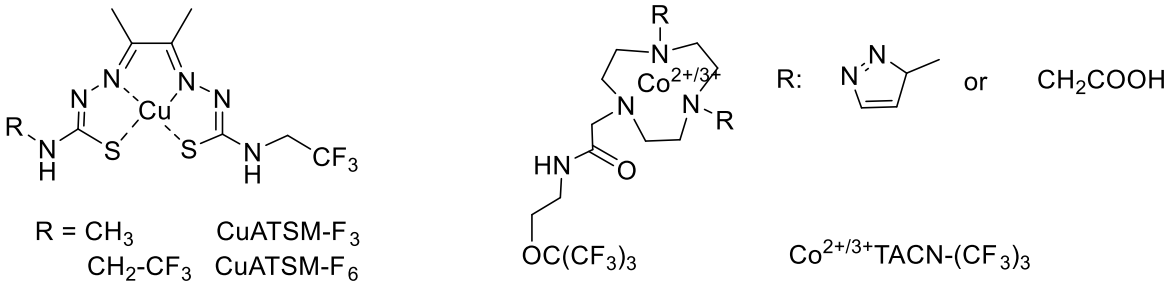

Scheme 9. Responsive ^{19}F probes based on transition metal complexes.

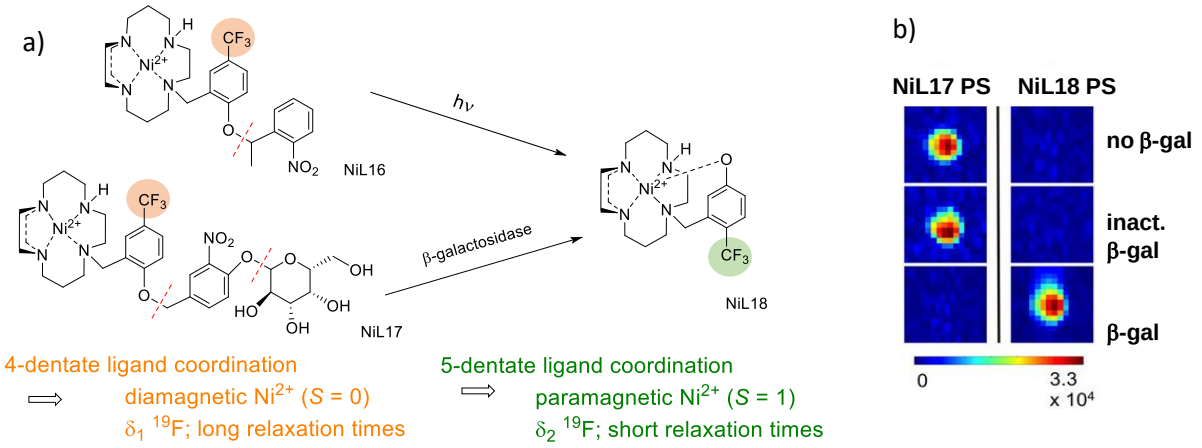

Figure 5. a) Spin state switching of Ni^{2+} is induced by ligand coordination change. b) Detection of *in vitro* β-galactosidase activity through ^{19}F NMR. Phantom images were obtained at 7 T, with RARE pulse sequences (PS) adapted for NiL17 or NiL18, respectively. Adapted with permission from Ref. [57]

Conclusions and perspectives

This short review describes some recent advances in the design of biochemically responsive, metal-based MRI agents. We highlight smart probes for MRI mapping of biologically relevant metal ions, and transition metal complexes with MRI response to various biomarkers. Concentrations of Ca^{2+}, Zn^{2+} and Cu^{2+} in certain tissues are high enough (~10 μM-mM range) to be accessible for MRI detection, and they show considerable variations depending on the site and its physio-pathological state. After fifteen years of chemistry efforts with limited *in vivo* translation, today there is an increasing number of successful preclinical applications of metal-based agents to visualize Ca^{2+}, Zn^{2+} or Cu^{2+} concentrations. In parallel, a growing body of physical-chemical data help the fine understanding of their structure-activity relationships, facilitating further molecular optimization.

The search to replace Gd^{3+} with more biocompatible transition metal alternatives was first of all promoted by the toxicity concerns linked to this lanthanide ion. By now, it has become obvious that the very versatile coordination chemistry, magnetic and redox properties of transition metals ions such as $Mn^{2+/3+}$, $Fe^{2+/3+}$, $Co^{2+/3+}$, $Cu^{+/2+}$ and others offer unprecedented opportunities to the chemists to derive probes that can provide MRI detectable responses to biomarkers. Responsive MR imaging is also increasingly extended beyond traditional relaxation-based ^{1}H detection and takes further benefit from the frequency-encoded nature of paraCEST or parashift techniques.

[1] A. Merbach, L. Helm, E. Toth, The Chemistry of Contrast Agents in Medical Magnetic resonance Imaging, Second Edition ed., John Wiley & Sons, Chichester, 2013.
[2] J. Wahsner, E.M. Gale, A. Rodríguez-Rodríguez, P. Caravan:**Chemistry of MRI Contrast Agents: Current Challenges and New Frontiers**. *Chem. Rev.* 2018.
[3] T. Grobner:**Gadolinium - a specific trigger for the development of nephrogenic fibrosing dermopathy and nephrogenic systemic fibrosis?** *Neph. Dial. Transp.* 2006, **21:** 1104-1108.
[4] C.S. Bonnet:**Zn2+ detection by MRI using Ln3+-based complexes: The central role of coordination chemistry**. *Coord. Chem. Rev.* 2018, **369:** 91-104.
[5] L. Connah, V. Truffault, C. Platas-Iglesias, G. Angelovski:**Investigations into the effects of linker length elongation on the behaviour of calcium-responsive MRI probes**. *Dalton Trans.* 2019, **48:** 13546-13554.
[6] F. Garello, S. Gunduz, S. Vibhute, G. Angelovski, E. Terreno:**Dendrimeric calcium-sensitive MRI probes: the first low-field relaxometric study**. *J. Mat. Chem. B* 2020, **8:** 969-979.
[7] A.F. Martins, V.C. Jordan, F. Bochner, S. Chirayil, N. Paranawithana, S. Zhang, S.-T. Lo, X. Wen, P. Zhao, M. Neeman, A.D. Sherry:**Imaging Insulin Secretion from Mouse Pancreas by MRI Is Improved by Use of a Zinc-Responsive MRI Sensor with Lower Affinity for Zn2+ Ions**. *J. Am. Chem. Soc.* 2018, **140:** 17456-17464.
[8] M. Isaac, A. Pallier, F. Szeremeta, P.-A. Bayle, L. Barantin, C.S. Bonnet, O. Seneque:**MRI and luminescence detection of Zn2+ with a lanthanide complex-zinc finger peptide conjugate**. *Chem. Commun.* 2018, **54:** 7350-7353.
** An original design of Zn^{2+} responsive probe: a bioinspired system based on a on azinc finger peptide active both in MRI and luminescence*
[9] M. Bödenler, L. de Rochefort, P.J. Ross, N. Chanet, G. Guillot, G.R. Davies, C. Gösweiner, H. Scharfetter, D.J. Lurie, L.M. Broche:**Comparison of fast field-cycling magnetic resonance imaging methods and future perspectives**. *Mol. Phys.* 2019, **117:** 832-848.
[10] J.K. Alford, B.K. Rutt, T.J. Scholl, W.B. Handler, B.A. Chronik:**Delta Relaxation Enhanced MR: Improving Activation-Specificity of Molecular Probes through R-1 Dispersion Imaging**. *Magn. Reson. Med.* 2009, **61:** 796-802.
[11] M. Bödenler, K.P. Malikidogo, J.-F. Morfin, C.S. Aigner, É. Tóth, C.S. Bonnet, H. Scharfetter:**High-Field Detection of Biomarkers with Fast Field-Cycling MRI: The Example of Zinc Sensing**. *Chem. Eur. J.* 2019, **25:** 8236-8239.
** The use of fast-field cycling MRI to detect Zn^{2+} at high field, which was impossible using classical MRI methods*
[12] A.J.M. Lubag, L.M. De Leon-Rodriguez, S.C. Burgess, A.D. Sherry:**Noninvasive MRI of beta-cell function using a Zn2+-responsive contrast agent**. *Proc. Natl. Acad. Sci. USA* 2011, **108:** 18400-18405.
** The first in vivo study proving the feasability of Zn2+ detection
[13] T. Savic, G. Gambino, V.S. Bokharaie, H.R. Noori, N.K. Logothetis, G. Angelovski:**Early detection and monitoring of cerebral ischemia using calcium-responsive MRI probes**. *Proc. Natl. Acad. Sci. USA* 2019, **116:** 20666-20671.
*** In vivo Ca^{2+} detection by MRI using a responsive contrast agent during cerebral ischemia*
[14] M.V.C. Jordan, S.-T. Lo, S. Chen, C. Preihs, S. Chirayil, S. Zhang, P. Kapur, W.-H. Li, L.M. De Leon-Rodriguez, A.J.M. Lubag, N.M. Rofsky, A.D. Sherry:**Zinc-sensitive MRI contrast agent detects differential release of Zn(II) ions from the healthy vs. malignant mouse prostate**. *Proc. Natl. Acad. Sci. USA* 2016, **113:** E5464-E5471.
[15] V. Clavijo Jordan, A. Al-Ebraheem, K. Geraki, E. Dao, A.F. Martins, S. Chirayil, M. Farquharson, A.D. Sherry:**Synchrotron Radiation X-ray Fluorescence Elemental Mapping in Healthy versus Malignant Prostate Tissues Provides New Insights into the Glucose-Stimulated Zinc Trafficking in the Prostate As Discovered by MRI**. *Inorg. Chem.* 2019, **58:** 13654-13660.

[16] N.N. Paranawithana, A.F. Martins, V. Clavijo Jordan, P. Zhao, S. Chirayil, G. Meloni, A.D. Sherry:**A Responsive Magnetic Resonance Imaging Contrast Agent for Detection of Excess Copper(II) in the Liver In Vivo**. *J. Am. Chem. Soc.* 2019, **141:** 11009-11018.
[17] K.P. Malikidogo, I. Da Silva, J.-F. Morfin, S. Lacerda, L. Barantin, T. Sauvage, J. Sobilo, S. Lerondel, E. Toth, C.S. Bonnet:**A cocktail of 165Er(iii) and Gd(iii) complexes for quantitative detection of zinc using SPECT and MRI**. *Chem. Commun.* 2018, **54:** 7597- 7600.
** The first example of cation quantification by MRI and TEMP requiring the use of a non classical radioisotope*
[18] M. Le Fur, N.J. Rotile, C. Correcher, V.C. Jordan, A.W. Ross, C. Catana, P. Caravan:**Yttrium-86 Is a Positron Emitting Surrogate of Gadolinium for Noninvasive Quantification of Whole-Body Distribution of Gadolinium-Based Contrast Agents**. *Angew. Chem. Int. Ed.* 2020, **59:** 1474-1478.
[19] G. Gambino, T. Gambino, G. Angelovski:**Combination of bioresponsive chelates and perfluorinated lipid nanoparticles enables in vivo MRI probe quantification**. *Chem. Commun.* 2020, **56:** 9433-9436.
[20] K. Srivastava, G. Ferrauto, S.M. Harris, D.L. Longo, M. Botta, S. Aime, V.C. Pierre:**Complete on/off responsive ParaCEST MRI contrast agents for copper and zinc**. *Dalton Trans.* 2018, **47:** 11346-11357.
[21] A.C. Harnden, D. Parker, N.J. Rogers:**Employing paramagnetic shift for responsive MRI probes**. *Coord. Chem. Rev.* 2019, **383:** 30-42.
[22] A.C. Harnden, A.S. Batsanov, D. Parker:**Paramagnetic Lanthanide NMR Probes Signalling Changes in Zinc Concentration by Emission and Chemical Shift: A Proof of Concept Study**. *Chem. Eur. J.* 2019, **25:** 6212-6225.
*** The first example of cation detection using parashift pobe*
[23] M. Yu, D. Xie, R.T. Kadakia, W. Wang, E.L. Que:**Harnessing chemical exchange:F-19 magnetic resonance OFF/ON zinc sensing with a Tm(iii) complex**. *Chem. Commun.* 2020, **56:** 6257-6260.
[24] G. Gambino, T. Gambino, R. Pohmann, G. Angelovski:**A ratiometric F-19 MR-based method for the quantification of Ca2+ using responsive paramagnetic probes**. *Chem. Commun.* 2020, **56:** 3492-3495.
[25] E. Kanal, M.F. Tweedle:**Residual or Retained Gadolinium: Practical Implications for Radiologists and Our Patients**. *Radiology* 2015, **275:** 630-634.
[26] A. Gupta, P. Caravan, W.S. Price, C. Platas-Iglesias, E.M. Gale:**Applications for Transition-Metal Chemistry in Contrast-Enhanced Magnetic Resonance Imaging**. *Inorg. Chem.* 2020, **59:** 6648-6678.
**A recent review on the use of transition metal complexes in MRI.*
[27] E.M. Gale, I.P. Atanasova, F. Blasi, I. Ay, P. Caravan:**A Manganese Alternative to Gadolinium for MRI Contrast**. *J. Am. Chem. Soc.* 2015, **137:** 15548-15557.
[28] R. Botar, E. Molnar, G. Trencsenyi, J. Kiss, F.K. Kalman, G. Tircso:**Stable and Inert Mn(II)-Based and pH-Responsive Contrast Agents**. *J. Am. Chem. Soc.* 2020, **142:** 1662-1666.
*** The first Mn^{2+}-based pH sensor with very high kinetic inertness.*
[29] F.K. Kálmán, V. Nagy, B. Váradi, Z. Garda, E. Molnár, G. Trencsényi, J. Kiss, S. Même, W. Même, É. Tóth, G. Tircsó:**Mn(II)-Based MRI Contrast Agent Candidate for Vascular Imaging**. *Journal of Medicinal Chemistry* 2020, **63:** 6057-6065.
[30] D. Ndiaye, M. Sy, A. Pallier, S. Meme, I. de Silva, S. Lacerda, A.M. Nonat, L.J. Charbonniere, E. Toth:**Unprecedented kinetic inertness for a Mn2+-bispidine chelate: a novel structural entry for Mn2+-based imaging agents**. *Angew. Chem. Int. Ed.* 2020, **59:** 11958-11963.
[31] J. Chen, W.-J. Zhang, Z. Guo, H.-B. Wang, D.-D. Wang, J.-J. Zhou, Q.-W. Chen:**pH-Responsive Iron Manganese Silicate Nanoparticles as T1-T2* Dual-Modal Imaging Probes for Tumor Diagnosis**. *ACS Appl. Mat. Int.* 2015, **7:** 5373-5383.
[32] G.A. Rolla, L. Tei, M. Fekete, F. Arena, E. Gianolio, M. Botta:**Responsive Mn(II) complexes for potential applications in diagnostic Magnetic Resonance Imaging**. *Bioorg. Med. Chem.* 2011, **19:** 1115-1122.
[33] T. Atanasijevic, X.-a. Zhang, S.J. Lippard, A. Jasanoff:**MRI Sensing Based on the Displacement of Paramagnetic Ions from Chelated Complexes**. *Inorg. Chem.* 2010, **49:** 2589-2591.

[34] Y. You, E. Tomat, K. Hwang, T. Atanasijevic, W. Nam, A.P. Jasanoff, S.J. Lippard:**Manganese displacement from Zinpyr-1 allows zinc detection by fluorescence microscopy and magnetic resonance imaging**. *Chem. Commun.* 2010, **46:** 4139-4141.
[35] M. Yu, M.B. Ward, A. Franke, S.L. Ambrose, Z.L. Whaley, T.M. Bradford, J.D. Gorden, R.J. Beyers, R.C. Cattley, I. Ivanović-Burmazović, D.D. Schwartz, C.R. Goldsmith:**Adding a Second Quinol to a Redox-Responsive MRI Contrast Agent Improves Its Relaxivity Response to H2O2**. *Inorg. Chem.* 2017, **56:** 2812-2826.
[36] C. Carop, M.L. Garcia-Martin, M.P. Leal:**Manganese-Based Nanogels as pH Switches for Magnetic Resonance Imaging**. *Biomacromolecules* 2017, **18:** 1617-1623.
[37] A. Barandov, B.B. Bartelle, B.A. Gonzalez, W.L. White, S.J. Lippard, A. Jasanoff:**Membrane-Permeable Mn(III) Complexes for Molecular Magnetic Resonance Imaging of Intracellular Targets**. *J. Am. Chem. Soc.* 2016, **138:** 5483-5486.
[38] A. Barandov, B.B. Badelle, C.G. Williamson, E.S. Loucks, S.J. Lippard, A. Jasanoff:**Sensing intracellular calcium ions using a manganese-based MRI contrast agent**. *Nature Comm.* 2019, **10**.
***Visualisation of exclusively intracellular Ca^{2+} concentrations in the rat brain by a cell-penetrating Mn^{3+} complex.*

[39] A. Barandov, S. Ghosh, N. Li, B.B. Bartelle, J.I. Daher, M.L. Pegis, H. Collins, A. Jasanoff:**Molecular Magnetic Resonance Imaging of Nitric Oxide in Biological Systems**. *ACS Sens.* 2020, **5:** 1674-1682.
[40] S.M. Pinto, V. Tome, M.J.F. Calvete, M.M.C.A. Castro, E. Toth, C.F.G.C. Geraldes:**Metal-based redox-responsive MRI contrast agents**. *Coord. Chem. Rev.* 2019, **390:** 1-31.
[41] S. Aime, M. Botta, E. Gianolio, E. Terreno:**a p(O2)-Responsive MRI Contrast Agent Based on the Redox Switch of Manganese(II/III)-Porphyrin Complexes**. *Angew. Chem. Int. Ed.* 2000, **39:** 747-750.
[42] S.M.A. Pinto, V.A. Tome, M.J.F. Calvete, M.M. Pereira, H.D. Burrows, A.M.S. Cardoso, A. Pallier, M.M.C.A. Castro, E. Toth, C.F.G.C. Geraldes:**The quest for biocompatible phthalocyanines for molecular imaging: Photophysics, relaxometry and cytotoxicity studies**. *J. Inorg. Biochem.* 2016, **154:** 50-59.
[43] S.M.A. Pinto, M.J.F. Calvete, M.E. Ghica, S. Soler, I. Gallardo, A. Pallier, M.B. Laranjo, A.M.S. Cardoso, M.M.C.A. Castro, C.M.A. Brett, M.M. Pereira, E. Toth, C.F.G.C. Geraldes:**A biocompatible redox MRI probe based on a Mn(II)/Mn(III) porphyrin**. *Dalton Trans.* 2019, **48:** 3249-3262.
[44] E.M. Gale, C.M. Jones, I. Ramsay, C.T. Farrar, P. Caravan:**A Janus Chelator Enables Biochemically Responsive MRI Contrast with Exceptional Dynamic Range**. *J. Am. Chem. Soc.* 2016, **138:** 15861-15864.
** The first redox sensor where the chelate switches between two coordination modes in order to adapt to the redox state of Mn.*

[45] J. Han, G. Liang, D. Xing:**A pH-Sensitive Zwitterionic Iron Complex Probe with High Biocompatibility for Tumor-Specific Magnetic Resonance Imaging**. *Chem. Eur. J.* 2019, **25:** 8353-8362.
[46] H. Wang, V.C. Jordan, I.A. Ramsay, M. Sojoodi, B.C. Fuchs, K.K. Tanabe, P. Caravan, E.M. Gale:**Molecular Magnetic Resonance Imaging Using a Redox-Active Iron Complex**. *J. Am. Chem. Soc.* 2019, **141:** 5916-5925.
[47] C.J. Bond, R. Cineus, A.Y. Nazarenko, J.A. Spernyak, J.R. Morrow:**Isomeric Co(ii) paraCEST agents as pH responsive MRI probes**. *Dalton Trans.* 2020, **49:** 279-284.
[48] K. Srivastava, G. Ferrauto, V.G. Young, S. Aime, V.C. Pierre:**Eight-Coordinate, Stable Fe(II) Complex as a Dual 19F and CEST Contrast Agent for Ratiometric pH Imaging**. *Inorg. Chem.* 2017, **56:** 12206-12213.
[49] A.E. Thorarinsdottir, K. Du, J.H.P. Collins, T.D. Harris:**Ratiometric pH Imaging with a CoII2 MRI Probe via CEST Effects of Opposing pH Dependences**. *J. Am. Chem. Soc.* 2017, **139:** 15836-15847.
[50] K. Du, E.A. Waters, T.D. Harris:**Ratiometric quantitation of redox status with a molecular Fe2 magnetic resonance probe**. *Chem. Sci.* 2017, **8:** 4424-4430.
[51] D. Xie, M. Yu, R.T. Kadakia, E.L. Que:**19F Magnetic Resonance Activity-Based Sensing Using Paramagnetic Metals**. *Acc. Chem. Res.* 2020, **53:** 2-10.

[52] D. Xie, T.L. King, A. Banerjee, V. Kohli, E.L. Que:**Exploiting Copper Redox for 19F Magnetic Resonance-Based Detection of Cellular Hypoxia**. *J. Am. Chem. Soc.* 2016, **138:** 2937-2940.
[53] D. Xie, S. Kim, V. Kohli, A. Banerjee, M. Yu, J.S. Enriquez, J.J. Luci, E.L. Que:**Hypoxia-Responsive 19F MRI Probes with Improved Redox Properties and Biocompatibility**. *Inorg. Chem.* 2017, **56:** 6429-6437.
[54] J.S. Enriquez, M. Yu, B.S. Bouley, D. Xie, E.L. Que:**Copper(ii) complexes for cysteine detection using F-19 magnetic resonance**. *Dalton Trans.* 2018, **47:** 15024-15030.
[55] M. Yu, B.S. Bouley, D. Xie, J.S. Enriquez, E.L. Que:**19F PARASHIFT Probes for Magnetic Resonance Detection of H2O2 and Peroxidase Activity**. *J. Am. Chem. Soc.* 2018, **140:** 10546-10552.
[56] M. Yu, D. Xie, K.P. Phan, J.S. Enriquez, J.J. Luci, E.L. Que:**A Co-II complex for F-19 MRI-based detection of reactive oxygen species**. *Chem. Commun.* 2016, **52:** 13885-13888.
[57] D. Xie, M. Yu, Z.-L. Xie, R.T. Kadakia, C. Chung, L.E. Ohman, K. Javanmardi, E.L. Que:**Versatile Nickel(II) Scaffolds as Coordination-Induced Spin-State Switches for 19F Magnetic Resonance-Based Detection**. *Angew. Chem. Int. Ed.* 2020, **doi.org/10.1002/anie.202010587**

*** In cell proof-of-concept examples of inducing spin-switch of Ni^{2+} complexes by modulation of ligand coordination following interaction with a biomarker, for ^{19}F MRI detection.*